

## **Patient-Specific Mapping between Myocardium and Coronary Arteries using Myocardial Thickness Variation**

Dongjin Han

*Associate Professor, Department of Fire Safety, Kyung-Il university, Korea*  
*han@kiu.ac.kr*

### **Abstract**

*For precise cardiac diagnostics and treatment, we introduce a novel method for patient-specific mapping between myocardial and coronary anatomy, leveraging local variations in myocardial thickness. This complex system integrates and automates multiple sophisticated components, including left ventricle segmentation, myocardium segmentation, long-axis estimation, coronary artery tracking, and advanced geodesic Voronoi distance mapping. It meticulously accounts for variations in myocardial thickness and precisely delineates the boundaries between coronary territories according to the conventional 17-segment myocardial model. Each phase of the system provides a step-by-step approach to automate coronary artery mapping onto the myocardium. This innovative method promises to transform cardiac imaging by offering highly precise, automated, and patient-specific analyses, potentially enhancing the accuracy of diagnoses and the effectiveness of therapeutic interventions for various cardiac conditions.*

**Keywords:** *Cardiac diagnostics; Myocardial anatomy; Coronary artery mapping*

### **1. Introduction**

Cardiovascular diseases, prominently featuring coronary stenosis, persist as the global leader in mortality. Traditional diagnostic benchmarks, such as coronary angiography, have been esteemed as the gold-standard for assessing and localizing coronary lesions. The advent of fractional flow reserve (FFR), offering a physiological assessment of coronary stenosis by quantifying maximal achievable coronary flow despite stenosis presence, marked a significant advancement in cardiac diagnostics. Further innovation is evidenced by noninvasive FFR computed from CT (FFR-CT) and adenosine-induced stress myocardial perfusion imaging via dual-source CT at cardiac CT angiography, both underscoring potential in detecting regional ischemia in acute chest pain scenarios, thus enhancing myocardial perfusion defect identification [1].

Despite these advancements, a gap persists in accurately mapping the specific coronary arteries to corresponding myocardial segments, critical for pinpointing stenotic arteries. Current methodologies,

---

Manuscript Received: May. 6, 2024 / Revised: May. 13, 2024 / Accepted: May. 20, 2024

Corresponding Author: han@kiu.ac.kr

Tel: \*\*\* \_ \*\*\*\* \_ \*\*\*\*

Author's affiliation (Associate Professor , Department of Fire Safety, Kyung-Il university, Korea)

including the American Heart Association (AHA)'s standardized 17-segment model for tomographic imaging of the left ventricle (LV) [2], predominantly rely on population averages and thus falter due to considerable anatomical variations among individuals as shown in Figure 1. Recent initiatives have sought to mitigate these inaccuracies through patient-specific coronary artery mapping, yet these efforts have not fully accounted for variations in myocardial thickness—a factor potentially pivotal in delineating coronary territories with greater precision [3-4].

In response, this paper proposes an innovative method that integrates patient-specific variations in myocardial thickness into coronary artery mapping. By building upon and expanding the work of Termeer et al. [5], this study introduces a novel approach encompassing automatic myocardium segmentation, artery extraction, and tracking combined with advanced geodesic Voronoi distance mapping. In Termeer's work, they did not consider the variation of the myocardium. This method is designed to automate the mapping of coronary arteries onto the myocardium adapting the thickness variation of individual patient, thus offering a step-wise, highly precise solution for improving cardiac diagnostic and therapeutic interventions. Our approach not only promises to refine the granularity of cardiac imaging but also to enhance the efficacy of treatments for various cardiac conditions by offering a more accurate, patient-specific analysis.

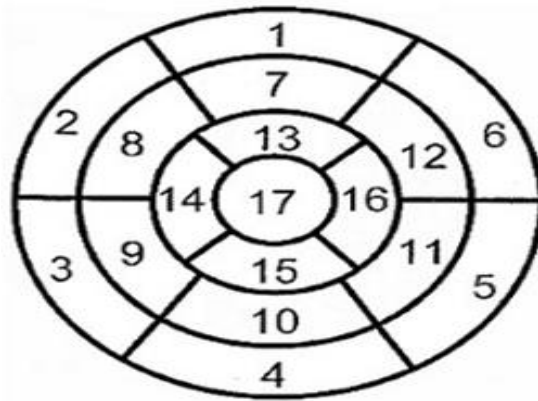


Figure 1. Bullseye map of left ventricular 17 myocardial segments

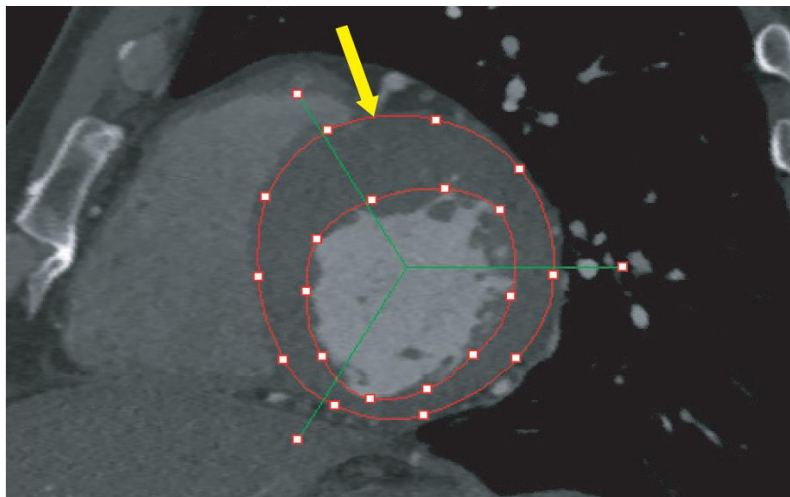


Figure 2. Example of segmentation. Arrow shows the thickest area.

## 2. Automatic Segmentation of Left Ventricle and Myocardium

A substantial body of research focuses on automatic cardiac and left ventricle segmentation using MRI or CT scans [6-11]. The segmentation of LV myocardium employs a level-set based method, where the endocardium and epicardium are initially estimated with B-spline contour points. Subsequently, operators may manually adjust these segmentation contours, if necessary, as shown in Figure 2, which depicts an image from the segmented volume. Echocardiography is the most widely used modality for the measurement of myocardium thickness. However, the regional 3D geometry of the normal human left ventricle can also be effectively achieved using CT images, allowing for the quantification of 3D regional myocardial wall thickening from gated magnetic resonance images. The thickness of the LV myocardium is measured by the distance between the epicardium and endocardium surfaces. After segmenting these two surfaces, for any given point on one surface, the nearest point on the other surface is determined, and the distance between these points is considered the thickness. Mathematically, if  $S_1$  and  $S_2$  represent the surfaces of the epicardium and endocardium, respectively, and  $P_{epi}$ ,  $P_{endo}$  are points on  $S_1$  and  $S_2$  then the nearest point  $P^*$  on  $S_2$  is found such that  $P^* = \min \text{norm} ||P_{epi}, P_{end}||$ .

## 3. Vessel Segmentation and Tracking

Extensive literature exists on artery tracking or reconstruction from CT or MRI data [12-14]. Traditional methods excel at tracking smaller vessels. In this research, our method for coronary artery tracking was used for general vessel tracking, which is three-dimensional and generates a 3D generalized cylinder model. Where bifurcation branching model can find small branches for complete coronary artery reconstruction [15]. Figure 3 left illustrates detected branch points of the coronary artery (LCX) marked with black circles. Figure 3 right image displays the center points of the left ventricle, indicating the need for a smooth axis. Thus, a quadratic 3D curve is fitted to these center points for axis regularization. It's crucial for the left anterior descending (LAD), left circumflex (LCX), and right coronary artery (RCA) to be mapped onto the left ventricular myocardium to construct a geodesic Voronoi map, taking into account the unique pathways and regions each artery supplies.

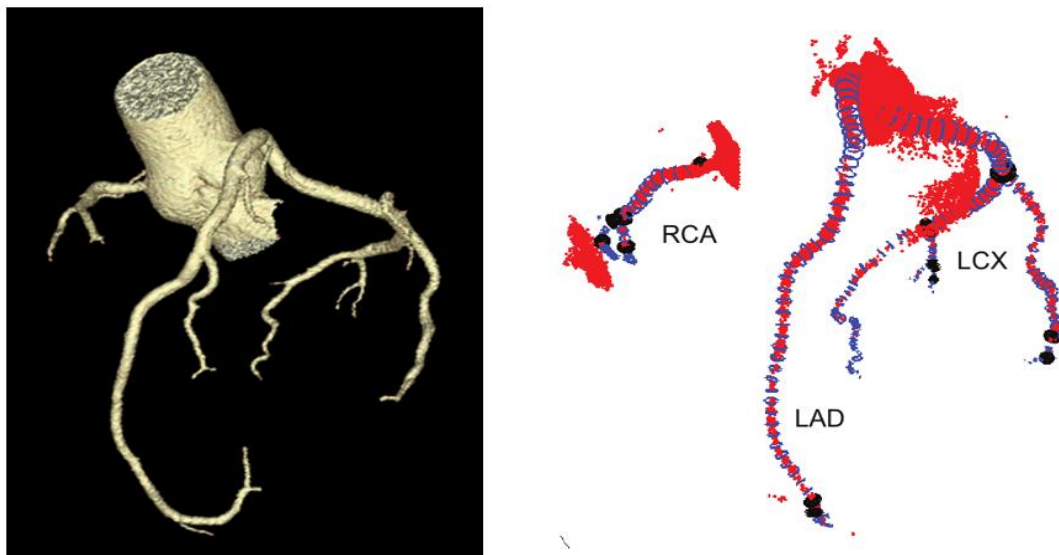


Figure 3. Coronary artery volume image and 3D geometric modeling

#### 4. Geodesic Voronoi Diagram on 3D Surface

Figure 4 illustrates the mapping of coronary arteries onto the left ventricle (LV) and their corresponding geodesic distance map. The Voronoi diagram of the primary coronary arteries is calculated using geodesic distances on the three-dimensional epicardium surface. The method employs the shortest paths for Riemannian manifold distance, known as geodesic distance, to address the segmentation mapping problem utilizing geodesic balls and Voronoi regions, sampling points at regular geodesic distances or meshing a domain with geodesic Delaunay triangles. The importance of geodesic distance lies in its adherence to significant curvilinear structures within the domain. The computation of numerical geodesic distances is used to identify the shortest paths across the left ventricle surface mesh. Depending on the mesh type, convergence might require more than 3000 iterations [18]. After calculating the geodesic distance on the 3D LV mesh, this distance helps in identifying boundaries where distances from different arteries are equal. Subsequently, these boundaries are depicted in a bullseye diagram.

This study posits that an increase in myocardium volume necessitates proportionally more blood flow, as represented by the volume increase. Accordingly, when a local myocardium region is thicker than others, it demands more blood flow, implying that the geodesic distance should be adjusted proportionally to the thickness increase. For instance, if the thickness increase of  $\Delta d_{th}$  at a point  $P$  on the epicardium will increase the volume proportional to square of  $\Delta d_{th}$ . Since the coverage of artery blood flows is proportional to the volume, the geodesic distance from the artery on the surface should decrease by  $-C\Delta dG$ , where  $C$  is a constant and  $dG \propto 1/\Delta d_{th}^2$ . This is illustrated in Figure 2 and Figure 6, where the yellow arrow denotes a thicker myocardium area, affecting the LAD-related geodesic distance.

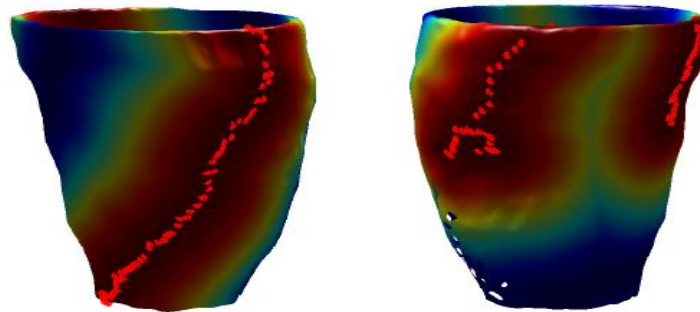


Figure 4. LAD and LCX mapping onto LV surface

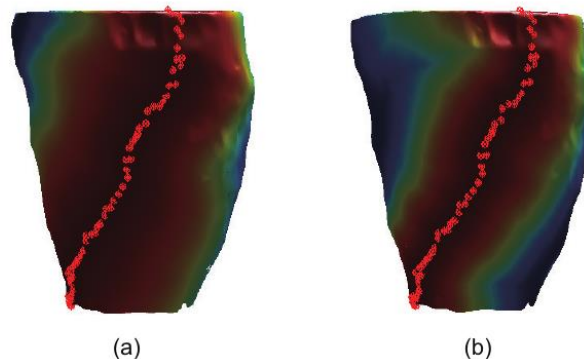


Figure 5. (a) LAD with local thickness not considered vs. (b) Considered

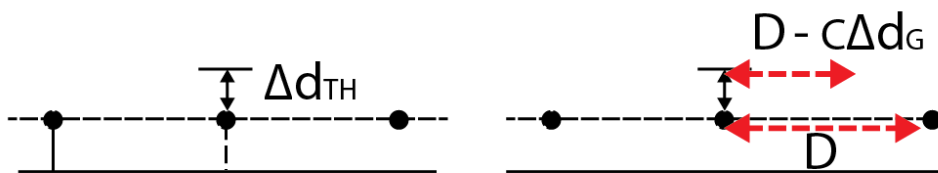


Figure 6. Myocardium thickness increase  $\Delta d_{TH}$  will shrink geodesic distance as  $C\Delta d_G$ .

## 5. Experiment

Our study meticulously mapped 3D reconstructed coronary arteries onto the epicardial surface, factoring in myocardial thickness into the mapping process. This innovative approach extends the epicardial surface in directions normal to each vertex, proportional to the myocardial thickness at that point, allowing for the computation of geodesic distances that are modulated by myocardial thickness. Figure 6 provides a comparative visualization, showcasing the impact of incorporating myocardial thickness on geodesic distances.

Figure 6 (b) reveals a crucial observation: as myocardial thickness increases, the associated geodesic distance decreases. This is a critical finding, affirming the hypothesis that regions with thicker myocardium—demanding more blood—should indeed occupy smaller geodesic distances in the coronary mapping. This adjustment ensures a more physiologically accurate representation of coronary artery territories, acknowledging the higher blood supply needs of thicker myocardial sections.

To illustrate the practical implications of our findings, we mapped the equidistance boundaries of coronary arteries onto a bullseye diagram, as seen in Figure 7. This visualization underscores the variation in coronary territories when myocardial thickness is considered, particularly evident in the diminished size of the LAD territory. Such observations are in line with our proposition that the myocardial thickness significantly influences coronary artery mapping, suggesting that thicker regions, which require increased blood flow, are accurately depicted with smaller geodesic distances in our model.

These results highlight the potential of integrating myocardial thickness into coronary artery mapping, promising to enhance the accuracy of cardiac diagnostics and treatment strategies. This nuanced understanding of coronary artery territories, adjusted for myocardial thickness, is poised to advance patient-specific cardiac care, particularly in the precise identification of ischemia-prone regions.

Future endeavors will aim to refine our model through clinical validation, further exploring how these detailed mappings can inform targeted treatment plans for cardiac patients. The adoption of this advanced mapping technique represents a significant leap towards personalized and effective cardiac healthcare.

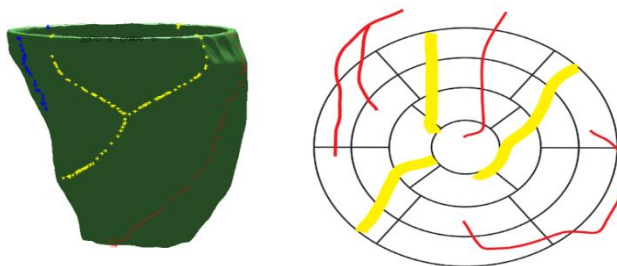
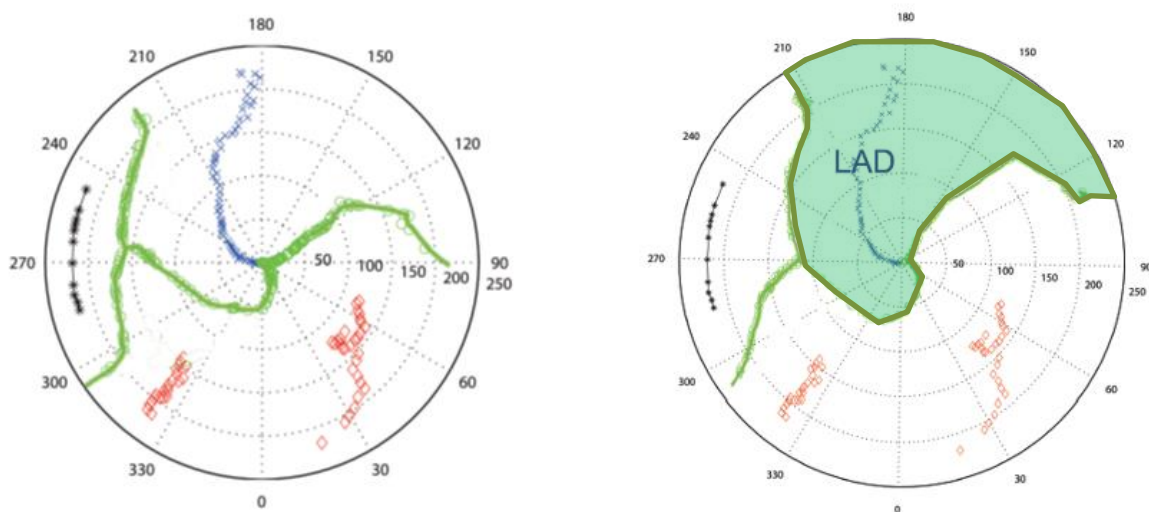


Figure 7. Equi-distance boundary of geodesic distance of coronary arteries (yellow) and its bullseye map. Red shows coronary artery mapping on the surface.



**Figure 8. Left: Without Myocardial thickness weight. Right: With Myocardial thickness weight. LAD mapping region shrinks.**

## 6. Discussion

This study introduces an innovative, automatic method for mapping coronary arteries onto the myocardium of the left ventricle, uniquely considering the local variations in myocardial thickness. Our preliminary findings suggest that the size of coronary territories decreases as the myocardial thickness in the corresponding regions increases. This correlation highlights the significance of incorporating myocardial thickness into models for a more accurate representation of coronary artery distribution. Our methodological framework encompasses myocardium segmentation, coronary artery tracking, and the application of a 3D geodesic Voronoi distance mapping technique. This approach facilitates a nuanced analysis of the coronary artery system, enabling the development of personalized cardiac diagnostics and treatment plans.

Further research will also explore several promising directions:

- Intensive medical verification is required to ensure the robustness of this method. Examining the role of the arterial radius in determining the distribution of coronary territories could add another layer of precision to our mapping technique.
- Developing techniques for detailed tracking and reconstruction of fine arterial structures could enhance the granularity and accuracy of coronary artery mapping.
- Investigating the application of our method to the mapping of the right coronary artery (RCA) onto the left ventricular myocardium may offer new perspectives on coronary circulation and myocardial blood supply.

## 7. Conclusion

Our study shows the potential for a deeper understanding of the intricate relationship between coronary artery anatomy and myocardial function. By addressing the aforementioned future research avenues, we aim to further the capabilities of cardiac imaging and treatment, ultimately contributing to improved outcomes for patients with cardiovascular diseases. Looking forward, we plan to conduct comprehensive clinical trials and animal studies to validate the efficacy and accuracy of our proposed method. The insights gained from these studies will be invaluable for refining our approach and ensuring its applicability in a clinical setting. This



innovative method promises to transform cardiac imaging by providing highly precise, automated, and patient-specific analyses, potentially improving the accuracy of diagnoses and the effectiveness of therapeutic interventions for various cardiac conditions.

## References

- [1] G. Bastarrika, L. Ramos-Duran, M. A. Rosenblum, D. K. Kang, G. W. Rowe, and U. J. Schoepf, "Adenosine-stress dynamic myocardial CT perfusion imaging: initial clinical experience," *Investigative Radiology*, vol. 45, no. 6, pp. 306–313, 2010.
- [2] M. D. Cerqueira, N. J. Weissman, V. Dilsizian, A. K. Jacobs, S. Kaul, W. K. Laskey, D. J. Pennell, J. A. Rumberger, T. Ryan, M. S. Verani, et al., "Standardized myocardial segmentation and nomenclature for tomographic imaging of the heart: a statement for healthcare professionals from the cardiac imaging committee of the council on clinical cardiology of the American Heart Association," *Circulation*, vol. 105, no. 4, pp. 539–542, 2002.
- [3] H. Kalbfleisch and W. Hort, "Quantitative study on the size of coronary artery supplying areas postmortem," *American Heart Journal*, vol. 94, no. 2, pp. 183–188, 1977.
- [4] Y. Koiwa, R. Bahn, and E. Ritman, "Regional myocardial volume perfused by the coronary artery branch: estimation in vivo," *Circulation*, vol. 74, no. 1, pp. 157–163, 1986.
- [5] M. Termeer, J. Bescos, M. Breeuwer, A. Vilanova, F. Gerritsen, E. Groller, and E. Nagel, "Patient-specific coronary artery supply territory AHA diagrams," *Journal of Cardiovascular Magnetic Resonance*, vol. 11, Suppl 1, p. P103, 2009.
- [6] M. Weininger, U. J. Schoepf, A. Ramachandra, C. Fink, G. W. Rowe, P. Costello, and T. Henzler, "Adenosine-stress dynamic real-time myocardial perfusion CT and adenosine-stress first-pass dual-energy myocardial perfusion CT for the assessment of acute chest pain: initial results," *European Journal of Radiology*, vol. 81, no. 12, pp. 3703–3710, 2012.
- [7] M. T. Dehkordi, S. Sadri, and A. Doosthoseini, "A review of coronary vessel segmentation algorithms," *J Med Signals Sens*, vol. 1, no. 1, pp. 49–54, 2011.
- [8] M. M. Hadhoud, M. I. Eladawy, A. Farag, F. M. Montevecchi, and U. Morbiducci, "Left ventricle segmentation in cardiac MRI images," *American Journal of Biomedical Engineering*, vol. 2, no. 3, pp. 131–135, 2012.
- [9] M. P. Jolly, "Automatic segmentation of the left ventricle in cardiac MR and CT images," *International Journal of Computer Vision*, vol. 70, no. 2, pp. 151–163, 2006.
- [10] M. R. Kaus, J. von Berg, J. Weese, W. Niessen, and V. Pekar, "Automated segmentation of the left ventricle in cardiac MRI," *Med Image Anal*, vol. 8, no. 3, pp. 245–254, 2004.
- [11] J. Lessick, Y. Fisher, R. Beyar, S. Sideman, M. L. Marcus, and H. Azhari, "Regional three-dimensional geometry of the normal human left ventricle using cine computed tomography," *Ann Biomed Eng*, vol. 24, no. 5, pp. 583–594, 1996.
- [12] D. Lesage, E. D. Angelini, I. Bloch, and G. Funka-Lea, "A review of 3D vessel lumen segmentation techniques: models, features, extraction schemes and algorithms," *Med Image Anal*, vol. 13, no. 6, pp. 819–845, 2009.
- [13] D. Marin, A. Aquino, M. Emilio Gegundez-Arias, and J. Manuel Bravo, "A new supervised method for blood vessel segmentation in retinal images by using gray-level and moment invariants-based features," *IEEE Transactions on Medical Imaging*, vol. 30, no. 1, pp. 146–158, 2011.
- [14] C. Kirbas and F. Quek, "A review of vessel extraction techniques and algorithms," *ACM Computing Surveys*, vol. 36, no. 2, pp. 81–121, 2004.
- [15] Dongjin Han et al., "Automatic coronary artery segmentation using active search for branches and seemingly disconnected vessel segments from coronary CT angiography," *PloS One*, vol. 118, e0156837, 18 Aug. 2016. <https://doi.org/10.1371/journal.pone.0156837>.
- [16] J. K. Min, J. Leipsic, M. J. Pencina, D. S. Berman, B.-K. Koo, C. van Mieghem, A. Erglis, F. Y. Lin, A. M. Dunning, P. Apruzzese, et al., "Diagnostic accuracy of fractional flow reserve from anatomic CT angiography: fractional flow reserve from CT angiography," *JAMA*, vol. 308, no. 12, pp. 1237–1245, 2012.

- [17] C. Petitjean and J. N. Dacher, "A review of segmentation methods in short axis cardiac MR images," *Med Image Anal*, vol. 15, no. 2, pp. 169–184, 2011.
- [18] G. Peyr e, M. Pechaud, R. Keriven, and L. Cohen, "Geodesic methods in computer vision and graphics," *Foundations and Trends in Computer Graphics and Vision*, vol. 5, nos. 3-4, pp. 197–397, 2010.
- [19] M. Prasad, A. Ramesh, P. Kavanagh, B. K. Tamarappoo, R. Nakazato, J. Gerlach, V. Cheng, L. E. Thomson, D. S. Berman, G. Germano, and P. J. Slomka, "Quantification of 3D regional myocardial wall thickening from gated magnetic resonance images," *J Magn Reson Imaging*, vol. 31, no. 2, pp. 317–327, 2010.
- [20] Shaaf ZF, Jamil MMA, Ambar R, Alattab AA, Yahya AA, Asiri Y. "Automatic left ventricle segmentation from short-axis cardiac MRI images based on fully convolutional neural network," *Diagnostics (Basel)*, vol. 12, no. 2, p. 414, 2022. <https://doi.org/10.3390/diagnostics12020414>.

**Sample Availability:** Samples of the compounds are available from the authors.

  2020 by the authors. Licensee MDPI, Basel, Switzerland. This article is an open access article distributed under the terms and conditions of the Creative Commons Attribution (CC BY

